chemistry proceedings

MDPI

Proceeding Paper

Functionalized Nanoparticles for Europium Recovery †

P. A. Martínez-Montoya [1,2*,†], J. M. del Río [1], A. de J. Morales-Ramirez [1,3], M. Corea [2], Jota Carrera Ma.-Luz [1] and T. Jiménez-Romero [1]

[1] Escuela Superior de Ingeniería Química e Industrias Extractivas, ESIQIE-IPN, Departamento de Ingeniería Metalúrgica UPALM S/N Col. Lindavista, Gustavo A. Madero, Ciudad de Mexico 07738, Mexico; email1@email.com (J.M.d.R.); email2@email.com (A.d.J.M.-R.); email3@email.com (J.C.M.-L.); email4@email.com (T.J.-R.)

[2] Escuela Superior de Ingeniería Química e Industrias Extractivas, ESIQIE-IPN, Laboratorio de Investigación en Polímeros y Nanomateriales, UPALM S/N Col. Lindavista, Gustavo A. Madero, Ciudad de Mexico 07738, Mexico; email5@email.com

[3] Centro de Investigación e Innovación Tecnológica, CIITEC-IPN, Cda. de CECATI, s/n, Santa Catarina, Azcapotzalco 02250, Mexico

* Correspondence: adrianpedrom@gmail.com

† Presented at the 27th International Electronic Conference on Synthetic Organic Chemistry (ECSOC-27), 15–30 November 2023; Available online: https://ecsoc-27.sciforum.net/.

Abstract: Polymeric nanoparticles of poly(methyl methacrylate) were obtained by emulsion polymerization techniques in a process of two stages. The synthesized particles were functionalized with acrylic acid, curcumin, and fumaramide and used to recovery of Eu from synthetic solutions. The nanoparticles showed excellent chelation capacity to trap rare-earth ions, because they recovered more than 85% of [Eu] at pH of 2, while they had a good stripping capacity, exceeding 50% of it. In addition, they had a homogeneity in morphology and good stability in dispersion for the recovery and stripping processes.

Keywords: [Eu] recovery; chelating effect; extraction process; stripping process

Citation: Martínez-Montoya, P.A.; del Río, J.M.; de J, A.; Corea, M.; Ma.-Luz, J.C.; Jiménez-Romero, T. Functionalized Nanoparticles for Europium Recovery. *Chem. Proc.* **2023**, *14*, x. https://doi.org/10.3390/xxxxx

Academic Editor(s): Name

Published: 10 November 2023

1. Introduction

The last decade has been developed new mechanisms for extraction to rare earths [1], principally by using organics extractants. These materials are expensive and highly polluting, and their complete replacement by compounds that improves the extraction and discharge efficiency, which are less polluting and more economical has not yet been achieved [2]. Currently, various adsorbents are used for rare earth ion recovery as: activated carbon, ion exchange resins [3], organic and inorganic composite materials, and biomaterials [4]. However, these materials often have low adsorption capacity and poor recyclability. Therefore, there is a necessity to synthesize new, efficient, and reliable materials for rare-earth recovery [2]. One proposal is the use of some functional groups that can adsorb or chelate a metal ion. The concept of the chelating effect must be understood as multivalency (or the use of multiple groups in combination to form a complex), which increases the strength and specificity of interaction [5]. There are reports on complexes of metal ions with various organic and inorganic ligands, where it has been shown that the strength of the association increases with the number of binding sites of the ligand to the metal ion [6]. The stability of the complex increases with several binding groups on the ligands, which is known as the chelation effect. These individual interactions of functional groups and metal ions are usually weak, which makes difficult to explain the high stability of the complexes. The binding of metal ions to the functional groups of the chelating agent facilitates the interaction of other ions with the other functional groups of the chelating agent, and therefore, these reagents are considered as concentrators of all these weak interactions in a small spatial region. This association can be considered an entropic

coordination, where a high concentration of functional groups covalently bound to the chelate increases the free energy of formation of interaction point [6]. Ethylenediaminetetraacetic acid (EDTA) is an example of chelating agent, because its ability to form stable complexes with divalent metal ions and a wide range of coordination ability. EDTA can form stable water-soluble chelates with almost all transition-metal ions [7]. EDTA and divalent metal ions form a chelate with multiple five-membered rings, where a carboxyl group is free, and a water molecule is coordinated with the metal center [8]. It complies with the coordination number of most metal ions because contains six coordination atoms. In general, the mixing ratio of chelates is 1:1. For this reason, EDTA is and therefore widely used in chemical analysis, synthetic detergents, the paper industry, biology, and metal ion remediation [9]. EDTA is not the only compound capable of forming complexes with metallic elements. For example, heavy metal ions can easily form complexes with ubiquitous substances such as citrate, nitrilotriacetic acid (NTA), cyanide, antibiotics, humic acid (HA), and other ligands to form stable metal complexes with varying structures and toxicities [10]. Impregnation and functionalization technology have been successfully applied to increase the adsorption capacity of polymeric adsorbents and enhance the ion exchange process by the effect of surface functional groups. An example is the poly(acrylic acid-co-acrylamide/16.16-dimethylheptadecan-1-amine P(AA-co-AM/PJM-T) used as an adsorbent for rare earth elements from monazite mineral and where its maximum adsorption capacity is 182.15 ± 3.73 mg/g at 25 °C [11]. Another approach to the recovery of rare earths is given by the development of organometallic structural materials functionalized with acrylic acid, repaired, and used for the selective adsorption of Rare Earth Elements (REE). The adsorption capacity of the material for Sc(III), Nd(III), Gd (III) and Er(III) was 90.21, 104.59, 58.29 and 74.94 mg/g, respectively [12]. Acrylic acid has also been successfully employed to treat effluents containing metal ions such as Co(II) or Ni(II) and was involved combined with poly(maleic acid) for the removal of chromium (III) [13]. Also, the use of curcumin in nanomaterials has been reported in the functionalization of copper oxide (CuO) nanoparticles by reflux and repeated doping with rare earth elements; lanthanum to prepare La-CuO, which were functionalized with curcumin. The new material was named Cu-La-CuO, for antimicrobial use with excellent effects, attributed to the incorporation of lanthanum and curcumin [14]. Other types of interactions between rare earth elements and curcumin have also been reported such as complexes of La, Nd, Pr, Ce, Eu and Sm, with curcumin in alcohol solution [15]. In addition to everything described above, it has been proven that curcumin forms complexes with many transition metals, such as copper, manganese, Co, Fe, V, Ga and In, and its metal complexes present potential for applications in medical, due to their therapeutic efficacy [15]. Fumaramide has also been reported to be used in hydrogel formation for cell encapsulation, with the function of improving or acquiring crosslinking capabilities in hydrogel particles [16]. As well as its application in induced polymerization in gel assemblies, where it was determined that the structure depends on the aggregates, in addition to the fact that the polymeric material can immobilize solvents [17]. As an answer to improve the recovery processes of rare earth elements, in particular europium and as an alternative to less polluting extraction mechanisms, this work proposes the synthesis of polymeric nanoparticles of poly(methyl methacrylate) (PMMA) functionalized with acrylic acid (AA), curcumin (CUR) and fumaramide (FA), where the functional group of each compound serves as adsorbent chelating the metal ion to forming metal complexes to recover europium. This could be an option to the traditional, polluting, and inefficient of recovery processes for rare earths.

2. Experimental Procedure

Extraction process and stripping of europium.

A synthetic europium solution was prepared from EuCl3·6H_2O, (Europium (III) chloride hexahydrate), supplied by Alfa Aesar, Reaction , 99.99% (REO, MA, USA) at 1000 ppm of [Eu] in aqueous media. For the extraction the previously prepared latex were mixed with the synthetic europium solution at 3 different latex-to-aqueous ratios 0.25, 0.5

and 1 (g of latex/10 mL of [Eu] aqueous solution) with constant agitation of 400 rpm for 120 min. At the end of the extraction time, the latex (loaded with metal ions) was separated from the aqueous surplus by centrifugation. The functional groups in the latex were not used in combination. The stripping was carried out with distilled water at different pH values (1.5, 6, and 9) modified with HCL drops. The used latex-aqueous ratio for the stripping was the same as for the extraction. Finally, a kinetic study was carried out of extraction and stripping processes at room temperature. The europium content of both processes was analyzed by atomic absorption spectrometry, AANALYS 200, Perkin Elmer (Waltham, MA, USA).

3. Results and Discussion

Three series of latex with different functional groups (AA, CUR and FA) were synthesized. The theoretical total solid content was changed in each one (5, 10 and 15 wt.%). The latex was analyzed by gravimetric techniques. The obtained results are presented in Table 1 and is observed that the experimental results are close to theoretical polymeric content.

Table 1. Experimental solid content in the synthesized latex.

Functional Groups	Total Solid Content		
	5 wt. %	**10 wt. %**	**15 wt. %**
AA	4.3 ± 0.1	8.5 ± 0.3	12.9 ± 0.3
CUR	3.8 ± 0.1	9.5 ± 0.4	14.0 ± 0.4
FA	4.0 ± 0.1	9.0 ± 0.2	13.0 ± 0.2

The particle size distribution of obtained latex were measured by DLS. From the data, number average diameter ($\overline{D_n}$); weight average diameter ($\overline{D_w}$), and Z-average ($\overline{D_z}$) were calculated using Equations (1)–(3) [18].

$$\overline{D_n} = \frac{\sum N_i D_i}{\sum N_i} \quad (1)$$

$$\overline{D_w} = \frac{\sum N_i {D_i}^4}{\sum N_i {D_i}^3} \quad (2)$$

$$\overline{D_z} = \frac{\sum N_i {D_i}^6}{\sum N_i {D_i}^5} \quad (3)$$

where N_i is the number of nanoparticles with diameter D_i

The polydispersity index (*PDI*) helps to understand the heterogeneity of a sample based on size and was calculated according to Equation (4), [19].

$$PDI = \frac{\overline{D_w}}{\overline{D_n}} \quad (4)$$

Table 2 shows the average Z-diameters ($\overline{D_z}$) of the particles and the polydispersity index of the obtained materials. The results show that all the latex had a polydispersity index of 1.1. This means, the particles are homogeneous and have almost the same diameter.

Table 2. Average particle size $\overline{D_Z}$ (nm) and polydispersity index (PDI) for materials with 5, 10 and 15 wt. % of polymer content.

wt. %	AA		CUR		FA	
	$\overline{D_Z}$ (nm)	PDI	$\overline{D_Z}$ (nm)	PDI	$\overline{D_Z}$ (nm)	PDI
5	121 ± 2	1.16	115 ± 2	1.18	161 ± 1	1.19
10	195 ± 4	1.18	233 ± 3	1.21	103 ± 2	1.18
15	99 ± 1	1.18	96 ± 0.1	1.19	94 ± 01	1.17

The latex series for each functional group with 15wt.% of solid content resulted to have the smaller particle size with an average of 96 ± 0.24 nm, followed by the series with 5 wt.% of solid content with an average of 133 ± 0.558 nm, while the series with 10 wt.% of polymer content resulted to have an average size of 177 ± 1.01 nm. In order to confirm these results, the morphology and size of the polymeric nanoparticles were observed by SEM. The images are presented in Figure 1, where is observed that the particles present a spherical morphology with a Gaussian size distribution, centered in all cases to 100 nm. The homogeneity of the nanoparticles is also observed; there is not agglomeration attributed to the crosslinking agent (EDGMA) used in the synthesis process [20]. In addition, monodisperse nanoparticles systems are also observed with a polydispersity index of 1.1.

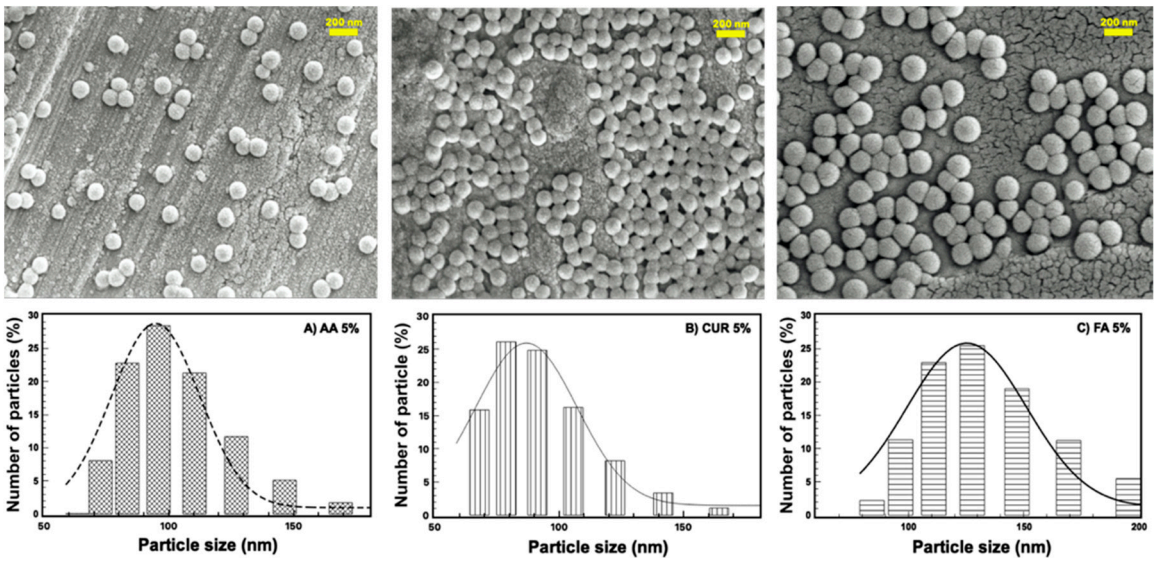

Figure 1. SEM images 50,000× of functionalized polymeric nanoparticles with (**A**) AA-5%, (**B**) CUR-5%, (**C**) FA-5%.

3.1. [Eu] Extraction Process

Figure 2 shows a synthesized scheme of the extraction process, where the interaction of the functional group (acrylic acid) with the metal ion is shown theoretically, as an example for the three-latex series. In the [Eu] extraction process, all latex series with different solid/liquid relations were tested. A latex ratio (1 g) with an aqueous volume of (10 mL) at a concentration of 1000 ppm of europium was mixed (solid/liquid ratio 0.1 g/mL). The initial pH of each solution containing the particles of latex functionalized was 2.7, 3.6, 3.75 for AA, CUR, and FA, respectively. An aliquot was taken from the aqueous supernatant of the mixture and was measured by atomic absorption. The results showed that the recovery of [Eu] is increased as the solid content in the latex is raised. The Figure 3 shows the percentage of europium recovered of the mixture at 120 min with constant agitation at room temperature.

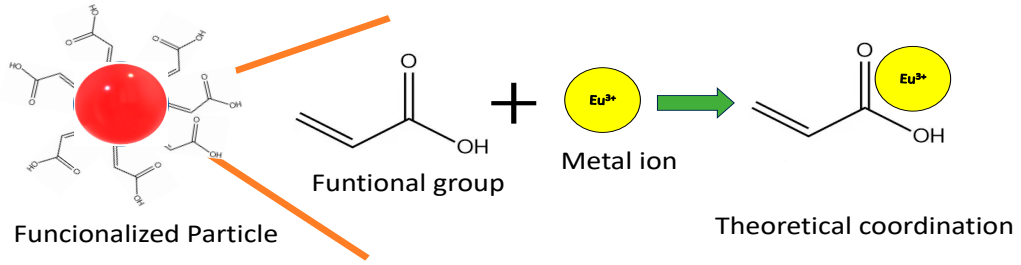

Figure 2. Synthesized scheme of the extraction process, with acrylic acid functionalized particles.

The results show that all materials functionalized with acrylic acid recovered more than 85% reaching until 98.04% of [Eu], while the latex with CUR and FA reached a maximum recovery of 84.90% and 45.20%, respectively when the polymer content was 15wt.%. Demonstrating, therefore that without the need to modify the initial pH, the best result is obtained with the highest solid/liquid ratio for this reason, only this ratio was used for subsequent experiments.

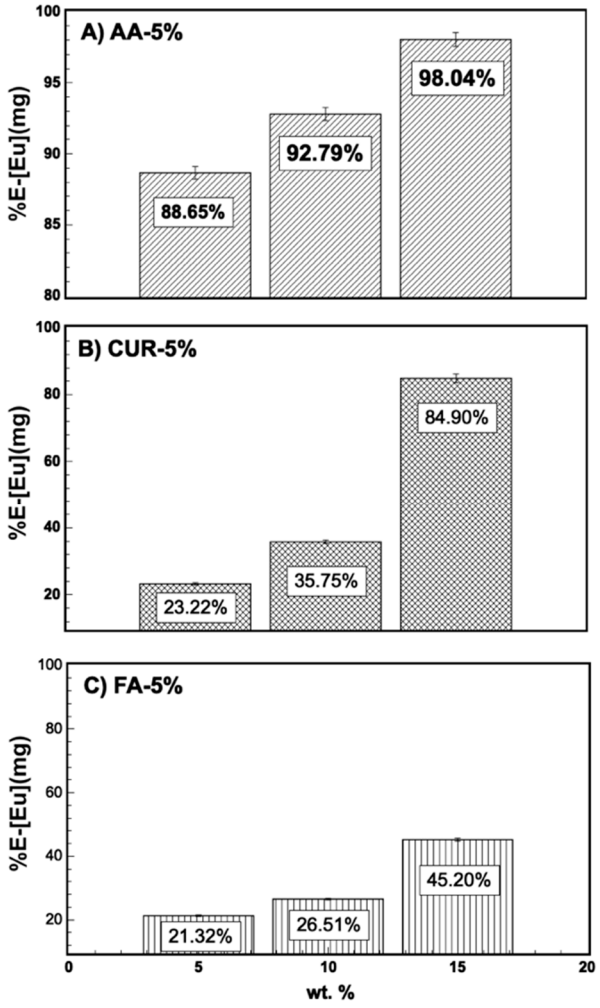

Figure 3. Extraction percentages of europium for the different series of latex. The same experimental conditions were maintained, and solid/liquid ratio was 0.1 g/mL, at an initial concentration of 1000 ppm of [Eu].

The high extraction efficiency [Eu] was obtained with acrylic acid series and can be attributed to different factors. The first is the initial pH of latex, because an acidic medium favors the extraction process. According to the Pourbaix diagram, the europium Eu^{3+}

exists at pH less than 7, E(v) = 0 [21]. This cation is attracted by the chelating effect that occurs by the carboxylic groups of the acrylic acid located on the surface of the nanoparticles. These functional groups together with the metal ion form a non-covalent complex called chelate. This chelating effect has been reported in other works, especially in the elaboration of hydrogels for the removal of heavy metals in wastewater where, by means of electrostatic attraction is gradually enhanced, resulting in a higher uptake of metal ions [22].

3.2. [Eu] Stripping Process

As a complementary advance to the application of functionalized polymeric nanoparticles after the extraction of the ions [Eu], they were submitted to a stripping process with distilled water (release of the trapped metal ions). For that, the pH was modified and the solid-liquid ratio 0.1 g/mL (1 g of latex per 10 mL of aqueous) maintained at same conditions of recovery process (120 min at room conditions). Thus, different pH values were used to identify the point of highest stripping (Figure 4) [21]. The results showed that 40% of [Eu] was released during the stripping process at pH 6. Considering that the initial concentration of [Eu] after the extraction process was 80% (800 mg/L-[Eu]) in a single work cycle at room conditions, the reached recovery percentage was 50%. This result could be improved by other work cycles at the same conditions.

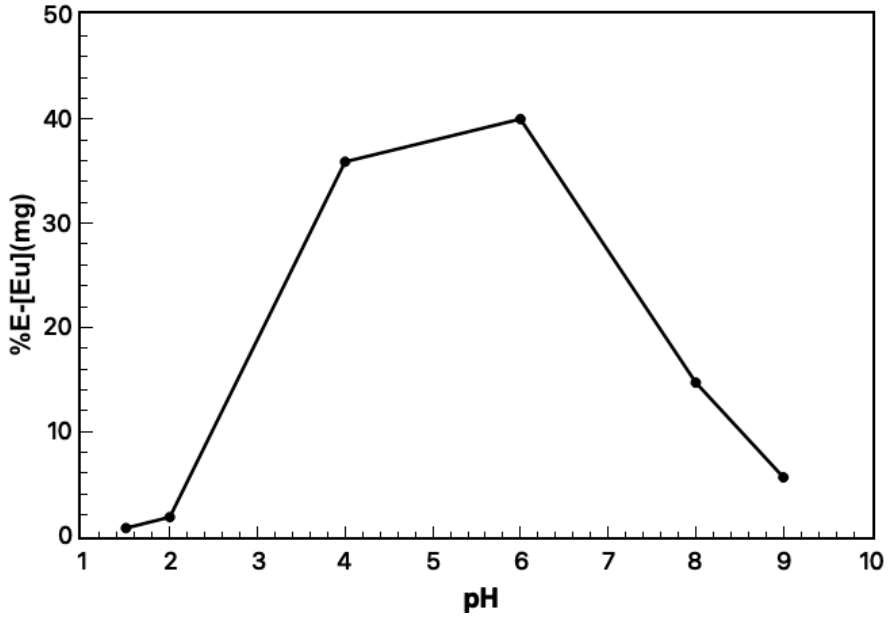

Figure 4. Stripping of [Eu] varying pH, 120 min, 1 g latex AA-15wt.% per 10 mL of aqueous. [Eu]-800 mg/L initial concentration.

4. Conclusions

Polymeric nanoparticles of PMMA functionalized with AA, CUR and FA, of homogeneous size (average 100 nm) and with good stability (ζ = −50 mV average) were obtained. The results of UV-vis and FT-IR confirmed the presence of functional groups on the surface of particle. The nanoparticles were applied to europium recovery process by solid-liquid extraction in two stages (extraction and stripping). For both stages the best conditions were determined as well as the compound with the highest affinity towards the europium metal ions. The pH lower than 2 was ideal for the extraction process with nanoparticles functionalized with acrylic acid and a solid-liquid ratio of 0.1 mg/mL; reaching recovery percentages higher than 85% (850 mg/L Eu). This behavior is attributed to the metal complex formation by the cooperative interaction between the functional groups to the attraction of [Eu] ion, called chelating effect. To stripping stage, at pH of 6 had a

higher release of metal ions, with a percentage of 50% in a single work cycle. According to the results, both processes followed a pseudo-second order kinetic model with a correlation coefficient of 0.98. Finally, by means of SEM and DLS it has been proved that the particles do not undergo morphological changes during the extraction and stripping processes of [Eu].

Acknowledgments: The nanoscience center of the IPN is acknowledged for the support provided during the development of the project.

Conflicts of Interest: The authors declare no conflict of interest. The funders had no role in the design of the study; in the collection, analyses, or interpretation of data; in the writing of the manuscript, or in the decision to publish the results.

References

1. Traore, M.; Gong, A.; Wang, Y.; Qiu, L.; Bai, Y.; Zhao, W.; Liu, Y.; Chen, Y.; Liu, Y.; Wu, H.; et al. Research progress of rare earth separation methods and technologies. *J. Rare Earths* **2023**, *41*, 182–189. https://doi.org/10.1016/j.jre.2022.04.009.
2. Hua, W.; Zhang, T.; Wang, M.; Zhu, Y.; Wang, X. Hierarchically structural PAN/UiO-66-(COOH)2 nanofibrous membranes for effective recovery of Terbium(III) and Europium(III) ions and their photoluminescence performances. *Chem. Eng. J.* **2019**, *370*, 729–741. https://doi.org/10.1016/j.cej.2019.03.255.
3. Chour, Z.; Laubie, B.; Morel, J.L.; Tang, Y.; Qiu, R.; Simonnot, M.O.; Muhr, L. Recovery of rare earth elements from Dicranopteris dichotoma by an enhanced ion exchange leaching process. *Chem. Eng. Process. —Process Intensif.* **2018**, *130*, 208–213. https://doi.org/10.1016/j.cep.2018.06.007.
4. Hisada, M.; Kawase, Y. Mucilage extracted from wasted natto (fermented soybeans) as a low-cost poly-γ-glutamic acid based biosorbent: Removal of rare-earth metal Nd from aqueous solutions. *J. Environ. Chem. Eng.* **2017**, *5*, 6061–6069. https://doi.org/10.1016/j.jece.2017.11.011.
5. Woodbury, C.P. Binding Sites. In *Introduction to Macromolecular Binding Equilibria*; CRC Press: Boca Raton, FL, USA, 2013. https://doi.org/10.1201/b12823-5.
6. Li, W.C.; Victor, D.M.; Chakrabarti, C.L. Effect of pH and Uranium Concentration on Interaction of Uranium(VI) and Uranium(IV) with Organic Ligands in Aqueous Solutions. *Anal. Chem.* **1980**, *52*, 520–523. https://doi.org/10.1021/ac50053a033.
7. Eivazihollagh, A.; Svanedal, I.; Edlund, H.; Norgren, M. On chelating surfactants: Molecular perspectives and application prospects. *J. Mol. Liq.* **2019**, *278*, 688–705. https://doi.org/10.1016/j.molliq.2019.01.076.
8. Shahid, M.; Austruy, A.; Echevarria, G.; Arshad, M.; Sanaullah, M.; Aslam, M.; Nadeem, M.; Nasim, W.; Dumat, C. EDTA-Enhanced Phytoremediation of Heavy Metals: A Review. *Soil Sediment Contam. Int. J.* **2014**, *23*, 389–416. https://doi.org/10.1080/15320383.2014.831029.
9. Zhu, Y.; Fan, W.; Zhou, T.; Li, X. Removal of chelated heavy metals from aqueous solution: A review of current methods and mechanisms. *Sci. Total. Environ.* **2019**, *678*, 253–266. https://doi.org/10.1016/j.scitotenv.2019.04.416.
10. Wang, T.; Cao, Y.; Qu, G.; Sun, Q.; Xia, T.; Guo, X.; Jia, H.; Zhu, L. Novel Cu(II)–EDTA Decomplexation by Discharge Plasma Oxidation and Coupled Cu Removal by Alkaline Precipitation: Underneath Mechanisms. *Environ. Sci. Technol.* **2018**, *52*, 7884–7891. https://doi.org/10.1021/acs.est.8b02039.
11. Ali, A.H.; Dakroury, G.A.; Hagag, M.S.; Abdo, S.M.; Allan, K.F. Sorption of Some Rare Earth Elements from Acidic Solution onto Poly(acrylic acid–co-acrylamide/16, 16-dimethylheptadecan-1-amine) Composite. *J. Polym. Environ.* **2022**, *30*, 1170–1188. https://doi.org/10.1007/s10924-021-02271-7.
12. Lou, Z.; Xiao, X.; Huang, M.; Wang, Y.; Xing, Z.; Xiong, Y. Acrylic Acid-Functionalized Metal–Organic Frameworks for Sc(III) Selective Adsorption. *ACS Appl. Mater. Interfaces* **2019**, *11*, 11772–11781. https://doi.org/10.1021/acsami.9b00476.
13. Muller, J.; Ding, X.; Geneste, A.; Zajac, J.; Prelot, B.; Monge, S. Complexation properties of water-soluble poly(vinyl alcohol) (PVA)-based acidic chelating polymers. *Sep. Purif. Technol.* **2021**, *255*, 117747. https://doi.org/10.1016/j.seppur.2020.117747.
14. Chakka, S.V.; Thanjavur, N.; Lee, S.; Kim, S. Synthesis and characterization of lanthanum-doped curcumin-functionalized antimicrobial copper oxide nanoparticles. *J. Rare Earths* **2022**, *41*, 1606–1615. https://doi.org/10.1016/j.jre.2022.08.020.
15. Li, D.; Liu, S.; Gu, L.; Li, G.; Ding, Y.; Dong, L. Preparation of rare earth complexes with curcumin and their stabilization for PVC. *Polym. Degrad. Stab.* **2021**, *184*, 109480. https://doi.org/10.1016/j.polymdegradstab.2020.109480.
16. Liang, N.; Flynn, L.E.; Gillies, E.R. Neutral, water-soluble poly(ester amide) hydrogels for cell encapsulation. *Eur. Polym. J.* **2020**, *136*, 109899. https://doi.org/10.1016/j.eurpolymj.2020.109899.
17. Gregorić, T.; Makarević, J.; Štefanić, Z.; Žinić, M.; Frkanec, L. Gamma Radiation- and Ultraviolet-Induced Polymerization of Bis(amino acid)fumaramide Gel Assemblies. *Polymers* **2022**, *14*, 214. https://doi.org/10.3390/polym14010214.
18. Buendía, S.; Cabañas, G.; Álvarez-Lucio, G.; Montiel-Sánchez, H.; Navarro-Clemente, M.; Corea, M. Preparation of magnetic polymer particles with nanoparticles of Fe(0). *J. Colloid Interface Sci.* **2011**, *354*, 139–143. https://doi.org/10.1016/j.jcis.2010.09.076.
19. A. Shrivastava, *Introduction to Plastics Engineering*. 2018. https://doi.org/10.1016/C2014-0-03688-X.
20. Rafieian, S.; Mirzadeh, H.; Mahdavi, H.; Masoumi, M.E. A review on nanocomposite hydrogels and their biomedical applications. *Sci. Eng. Compos. Mater.* **2019**, *26*, 154–174. https://doi.org/10.1515/secm-2017-0161.

21. Chen, Y.; Sun, P. pH-sensitive polyampholyte microgels of poly(acrylic acid-co-vinylamine) as injectable hydrogel for controlled drug release. *Polymers* **2019**, *11*, 285. https://doi.org/10.3390/polym11020285.
22. Ashrafizadeh, M.; Tam, K.C.; Javadi, A.; Abdollahi, M.; Sadeghnejad, S.; Bahramian, A. Synthesis and physicochemical properties of dual-responsive acrylic acid/butyl acrylate cross-linked nanogel systems. *J. Colloid Interface Sci.* **2019**, *556*, 313–323. https://doi.org/10.1016/j.jcis.2019.08.066